Journal of the Meteorological Society of Japan, Vol. 89, No. 4, pp. 341–361, 2011
DOI:10.2151/jmsj.2011-404

Migration Process and 3D Wind Field of Precipitation Systems Associated with a Diurnal Cycle in West Sumatera: Dual Doppler Radar Analysis during the HARIMAU2006 Campaign

Namiko SAKURAI

National Research Institute for Earth Science and Disaster Prevention, Tsukuba, Japan

Shuichi MORI

Research Institute for Global Change, JAMSTEC, Yokosuka, Japan

Masayuki KAWASHIMA, Yasushi FUJIYOSHI

Institute of Low Temperature Science, Hokkaido University, Sapporo, Japan

HAMADA Jun-Ichi

Research Institute for Global Change, JAMSTEC, Yokosuka, Japan

Shingo SHIMIZU

National Research Institute for Earth Science and Disaster Prevention, Tsukuba, Japan

Hironori FUDEYASU

Faculty of Education and Human Sciences, Yokohama National University, Yokohama, Japan

Yoshikazu TABATA

Research Institute for Sustainable Humanosphere, Kyoto University, Uji, Japan

Wendi HARJUPA

National Institute of Aeronautics and Space, Jakarta Pusat, Indonesia

Hiroyuki HASHIGUCHI

Research Institute for Sustainable Humanosphere, Kyoto University, Uji, Japan

Manabu D. YAMANAKA

SATREPS-MCCOE Promotion Office, Jakarta Pusat, Indonesia
Research Institute for Global Change, JAMSTEC, Yokosuka, Japan
DEPS-CPS, Kobe University, Kobe, Japan

Jun MATSUMOTO

Department of Geography, Tokyo Metropolitan University, Hachioji, Japan
Research Institute for Global Change, JAMSTEC, Yokosuka, Japan

EMRIZAL

Indonesian Meteorological and Geophysical Agency, Jakarta Pusat, Indonesia

Fadli SYAMSUDIN

Agency for the Assessment and Application of Technology, Jakarta Pusat, Indonesia

(Manuscript received 18 May 2010, in final form 31 May 2011)

Abstract

This study describes the three-dimensional structure and migration process of a westward-migrating precipitation system with a diurnal cycle observed on 10 November 2006 in west Sumatera as based on dual-Doppler radar analysis, rawinsonde data, and surface data. The location of convective cell generation over land in the daytime and the timing of an evening change in the migration direction of precipitation systems from landward to seaward were influenced by local circulation: in the morning, an isolated convective cell generated near the west coast propagated inland (toward the mountains) via the successive generation of new convective cells over the sea breeze. In the afternoon, convective cells in a precipitation system were generated over the western slopes of the mountains surrounding Lake Maninjau by thermally induced local circulation and the slope effect. In the evening, precipitation systems located over the mountains started to propagate toward the sea (westward) in response to a change in local circulation from landward to seaward winds. Subsequently, precipitation systems were newly generated over the sea near the west coast of Sumatera Island, merging with the systems that originated over land. These two sets of systems formed a larger system (long axis $>$ 100 km) than that over land (long axis of several tens of kilometers). The expanded precipitation system had a convective region with a long axis oriented parallel to the west coast of Sumatera Island and a short axis ($\sim$7 km) oriented perpendicular to the west coast at the leading edge of the system. The echo top height of the system was located at approximately 13 km and an anvil moved faster than the convective region above 6 km in height. The convergence was formed by an easterly wind component in the system and a southerly wind component over the sea around the leading edge of the system at the lowest layer. The expanded system migrated farther offshore at a speed of about 5 m s^{-1} via the self-replication of convective cells over the convergence at the leading edge of the system and via advection by ambient wind in the lower troposphere. The convergence regions at the leading edge of the system were continuously strengthened by downward transportation of horizontal momentum below 4 km, meaning that the system could be maintained for a long time and migrate offshore for a long distance.

1. Introduction

The Indonesian maritime continent, which is located in the equatorial tropics, is characterized by the world's largest amounts of rainfall and latent heat release (Ramage 1968). Heavy rainfall occurs over both land and the surrounding sea. A diurnal cycle of convective activity is one of the dominant phenomena in the tropics (Hendon and Woodberry 1993). There exists a distinct difference in the timing of the maximum in convective activity between land (evening) and sea (morning) areas within the Indonesian maritime continent (Murakami 1983; Nitta and Sekine 1994; Yang and Slingo 2001). The timing of the maximum in convective activity is delayed from the coastline to the sea off the coast (Yang and Slingo 2001).

The land-sea contrast in the timing of maximum convective activity over Sumatera Island is caused by the migration of cloud systems (Mori et al. 2004; Sakurai et al. 2005): convective activity becomes intense in the western part of Sumatera Island during the daytime and cloud systems migrate westward and eastward from this area for several hundred kilometers during the night, meaning that convection is active over the sea around Sumatera Island during the morning. Sakurai et al. (2005) reported that westward migration is more frequent than eastward migration. In addition, several studies have shown that annual rainfall over the sea in the vicinity of west Sumatera is much greater than that over the island itself, and that most of the heavy rainfall over the sea in this region occurs during nighttime (Hara et al. 2009; Mori et al. 2004; Wu et al. 2009). These studies speculated that the abundant rainfall over the sea near west Sumatera is related to the westward migration of precipitation systems. In these studies, two-dimensional and wide-range data collected by satellite systems such as Geostationary Meteorological Satellite (GMS) infrared-1 (IR1) and precipitation radar (PR) data from the Tropical Rainfall Measuring Mission (TRMM) were mainly used for analyses. However, these studies using satellite data did not clarify the mechanism of the migration of precipitation systems or the distinct difference in rainfall amount between land and sea. Consequently, it is necessary to perform ground based observations to capture the three-dimensional structure of migrating precipitation systems with a diurnal cycle at high temporal and spatial resolutions.

Several numerical studies using General Circulation

Corresponding author: Namiko Sakurai, National Research Institute for Earth Science and Disaster Prevention (NIED), 3-1, Tennodai, Tsukuba, Ibaraki 305-0006, Japan.
E-mail: sakurain@bosai.go.jp

Model (GCM), regional model, or Global Cloud Resolving Model (GCRM) have sought to simulate the diurnal cycle of convective activity throughout the Indonesian maritime continent (Arakawa and Kitoh 2005; Fujita et al. 2011; Hara et al. 2009; Neal and Slingo 2003; Sato et al. 2009; Wu et al. 2009). Unfortunately, the previous studies using GCMs did not adequately represent the phase of the diurnal cycle or the spatial distribution of precipitation: the simulated maximum precipitation is several hours earlier than that observed around the western coast of Sumatera Island and precipitation is much weaker than that observed over the sea near west Sumatera (Arakawa and Kitoh 2005; Hara et al. 2009; Neal and Slingo 2003). Neal and Slingo (2003) noted that the correct representation in a GCM of a diurnal cycle derived from migrating precipitation systems might lead to improvements in terms of the underestimated precipitation in the region. Recently, Wu et al. (2009), who used a regional model with nonhydrostatic and cloud system-resolving, succeeded in replicating the westward migration of precipitation systems with a diurnal cycle in the coastal region of west Sumatera. Using the regional model, the authors were able to simulate a more realistic precipitation distribution and phase of diurnal cycle than those of GCMs. In addition, Sato et al. (2009) and Fujita et al. (2011) reported that the spatial distribution of precipitation and the phase of diurnal cycle over Sumatera Island and its surrounding sea were realistically simulated by GCRM. These numerical studies suggested that a westward-migrating precipitation system with a diurnal cycle is a key factor in determining the spatial distribution of precipitation around the western coast of Sumatera Island. However, few observational studies have considered the three-dimensional structure and migration process of precipitation systems with a diurnal cycle in this region.

An X-band Doppler radar (XDR) was installed in mountainous terrain on Sumatera Island as part of the Coupling Process in the Equatorial Atmosphere (CPEA) project, which provided three-dimensional information on the internal structure of migrating precipitation systems with high temporal and spatial resolution (Fukao 2006; Kawashima et al. 2006; Sakurai et al. 2009). However, the XDR only covered the land area in west Sumatera, meaning that the internal structures of migratory precipitation systems over the sea remain unknown.

The Hydrometeorological ARray for ISV-Monsoon AUtomonitoring (HARIMAU) project, which operated from 2005 to 2010 (Yamanaka et al. 2008), involved an intensive observation campaign in west Sumatera between 26 October and 27 November 2006 (HARIMAU2006) using two XDRs that covered the sea area off the west coast of Sumatera Island, rawinsondes, and Equatorial Atmosphere Radar (EAR) (Fig. 1), yielding the three-dimensional wind field in westward-migrating precipitation systems with a diurnal cycle. The purpose of the present study is to describe the internal structure and migration process of a westward-migrating precipitation system with a diurnal cycle and to reveal the mechanism of the westward migration using HARIMAU2006 data. A westward-migrating precipitation system observed on 10 November 2006 is analyzed based on HARIMAU2006 data.

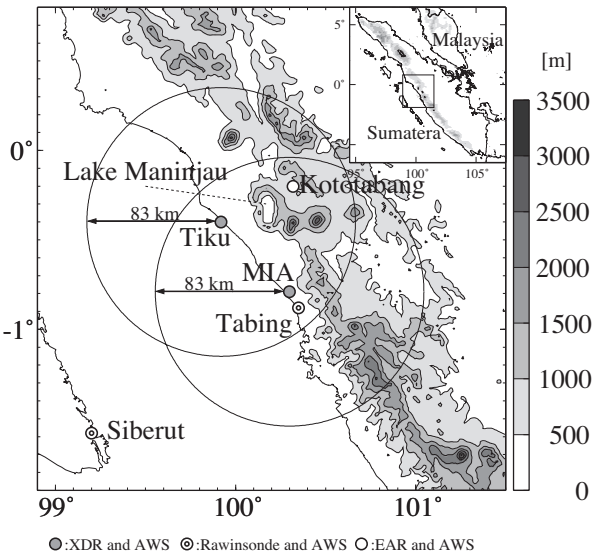

Fig. 1. Locations of two XDRs (MIA and Tiku), rawinsonde stations (Tabing and Siberut), and EAR (Kototabang) in west Sumatera Island with topography. AWSs were deployed at MIA, Tiku, Tabing, Siberut, and Kototabang. Two circles indicate the observation ranges (83 km) of the two XDRs located at MIA and Tiku. A box at the upper-right corner shows topography of Sumatera Island.

The remainder of this manuscript is organized as follows. Section 2 outlines the observations and data, and Section 3 presents a case study on the internal structure and temporal evolution of precipitation systems observed on 10 November 2006. Section 4 provides discussions on internal structure and migration mechanism of a westward-migrating precipitation system over the sea. Finally, the main findings of the study are summarized in Section 5.

Table 1. Major parameters of the X-band Doppler Radars (XDRs).

Items	Description	
	MIA	Tiku
Transmit frequency and polarization	9.770 GHz, Horizontal	9.445 GHz, Vertical
Transmit power	70 kW	40 kW
Beam width	0.98 deg	1.1 deg
Pulse width	0.5 μs	0.5 μs
Pulse repetition frequency	1,800 Hz	1,800 Hz
Antenna rotation speed	30 deg sec^{-1}	30 deg sec^{-1}
Rain detection range	83 km	83 km
Nyquist Velocity	13.8 m s^{-1}	16 m s^{-1}

2. Observations and data

Two XDRs were installed at Minangkabau International Airport (MIA) (100.30°E, 0.79°S) and Tiku (99.92°E, 0.40°S) in west Sumatera, Indonesia, in October 2006 as part of the HARIMAU project (Fig. 1). Figure 1 shows the topography and locations of observation stations in west Sumatera. In the observation area of the two XDRs, the coastline trends from northwest to southeast parallel to steep mountains in the eastern part of the observation area. Lake Maninjau (LM), a caldera lake, is located in the mountains within the observation area covered by the two XDRs. During HARIMAU2006, each XDR obtained volume scan data on reflectivity and Doppler velocity every 6 minutes within an 83 km radius (Table 1). The sampling resolution of XDR data was 200 m in the radial direction and 1.0° in the azimuthal direction. Each volume scan at MIA (Tiku) consisted of 18 (19) elevation angles from 0.5° to 50°. The Doppler velocity and reflectivity were interpolated into a Cartesian grid system with horizontal and vertical spacing of 0.5 km using a Cressman weighting function (Cressman 1959). Dual-Doppler analysis was performed using the variational method proposed by Shimizu et al. (2008). Several precipitation events were observed by the two XDRs during HARIMAU2006 (Mori et al. 2011). The present study analyzes a westward-migrating precipitation system observed on 10 November 2006 based on dual-Doppler data. Other precipitation events during HARIMAU2006 are analyzed with the two XDRs data by Fudeyasu et al. (2011) and Kawashima et al. (2011).

Intense rawinsonde observations were carried out at Tabing station of the Indonesian Meteorological and Geophysics Agency (BMG; now the Indonesian Meteorological Climatological and Geophysical Agency, BMKG) (100.35°E, 0.88°S) for 33 days (from 26 October to 27 November 2006) and at Siberut (Siberut National Park Office) (99.20°E, 1.58°S) for 11 days (4–14 November 2006) as part of HARIMAU2006 (Fig. 1).

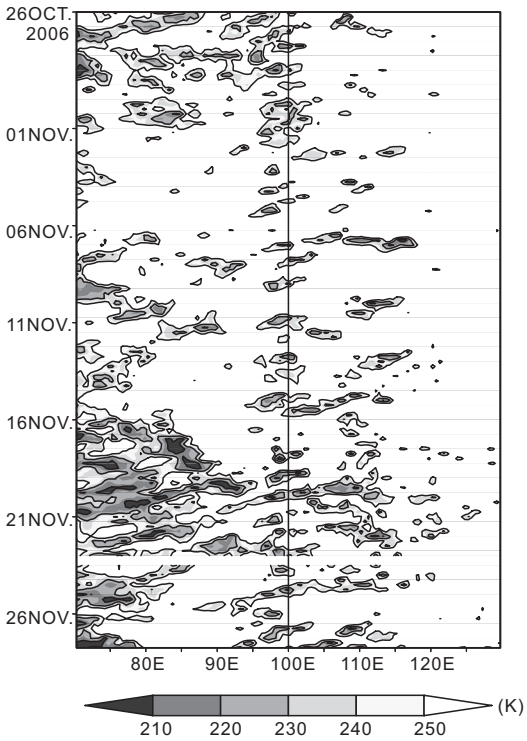

Fig. 2. Time-longitude cross-section of T_{BB} on the equator based on MTSAT IR1 data with a spatial resolution of 0.5°×0.5° between 26 October and 27 November 2006. Solid line indicates 100°E, which corresponds to the location of the central mountain range upon Sumatera Island, on the equator.

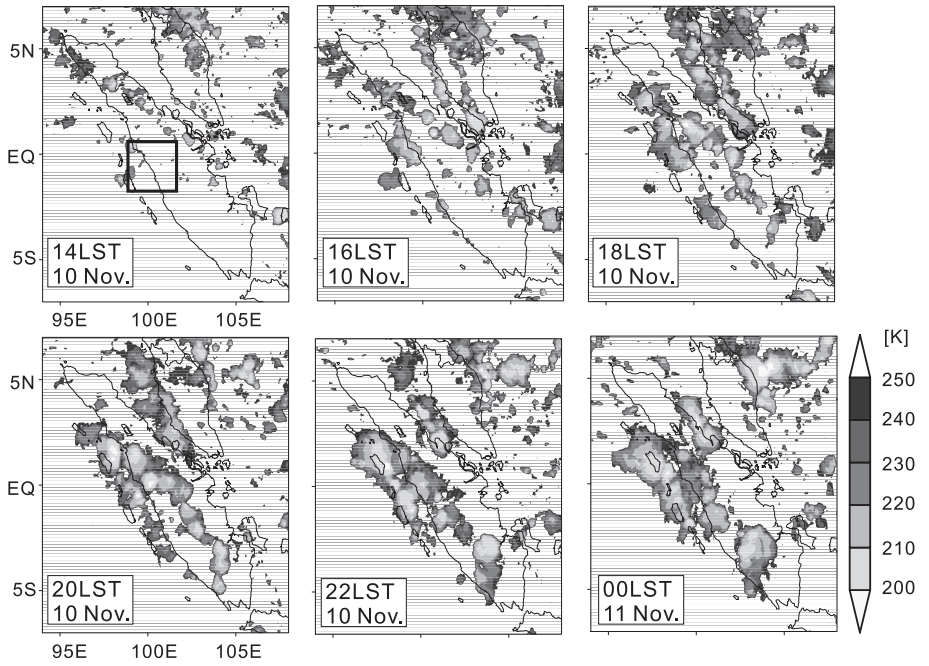

Fig. 3. Horizontal distributions of T_{BB} over Sumatera Island on 10 November 2006. The square at 1400 LST indicates the map area shown in Fig. 1.

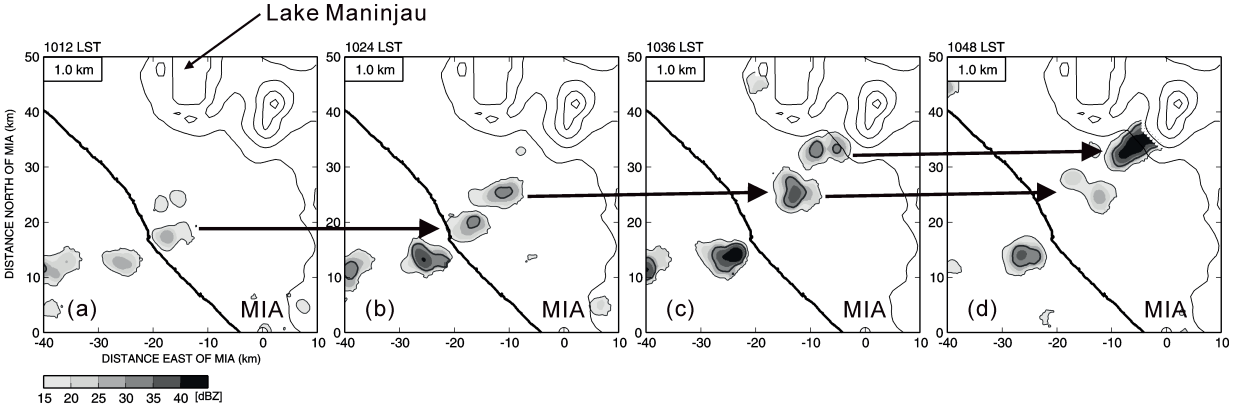

Fig. 4. Temporal variations in the horizontal distribution of precipitation systems at a height of 1.0 km from 1012 to 1048 LST on 10 November 2006. Thick and thin circles indicate 30 and 15 dBZ, respectively. The thick line indicates the coastline and contours show altitude at intervals of 500 m.

Rawinsonde data were obtained every 3 hours on 10 November 2006. We analyzed the rawinsonde data edited every 100 m in the vertical at Tabing. Surface data were obtained every minute during HARIMAU2006 at MIA, Tiku, Tabing, Siberut, and Kototabang using automatic weather stations (AWS). The present analysis employed data on wind speed and wind direction at the ground surface as observed at Tiku.

3. Structure and evolution of migratory cloud and precipitation systems

3.1 Temporal variations in the horizontal distribution of cloud systems

Climatologically, the period of HARIMAU2006 corresponded to one of two rainy seasons in central Sumatera (March-May and September-November; Hamada

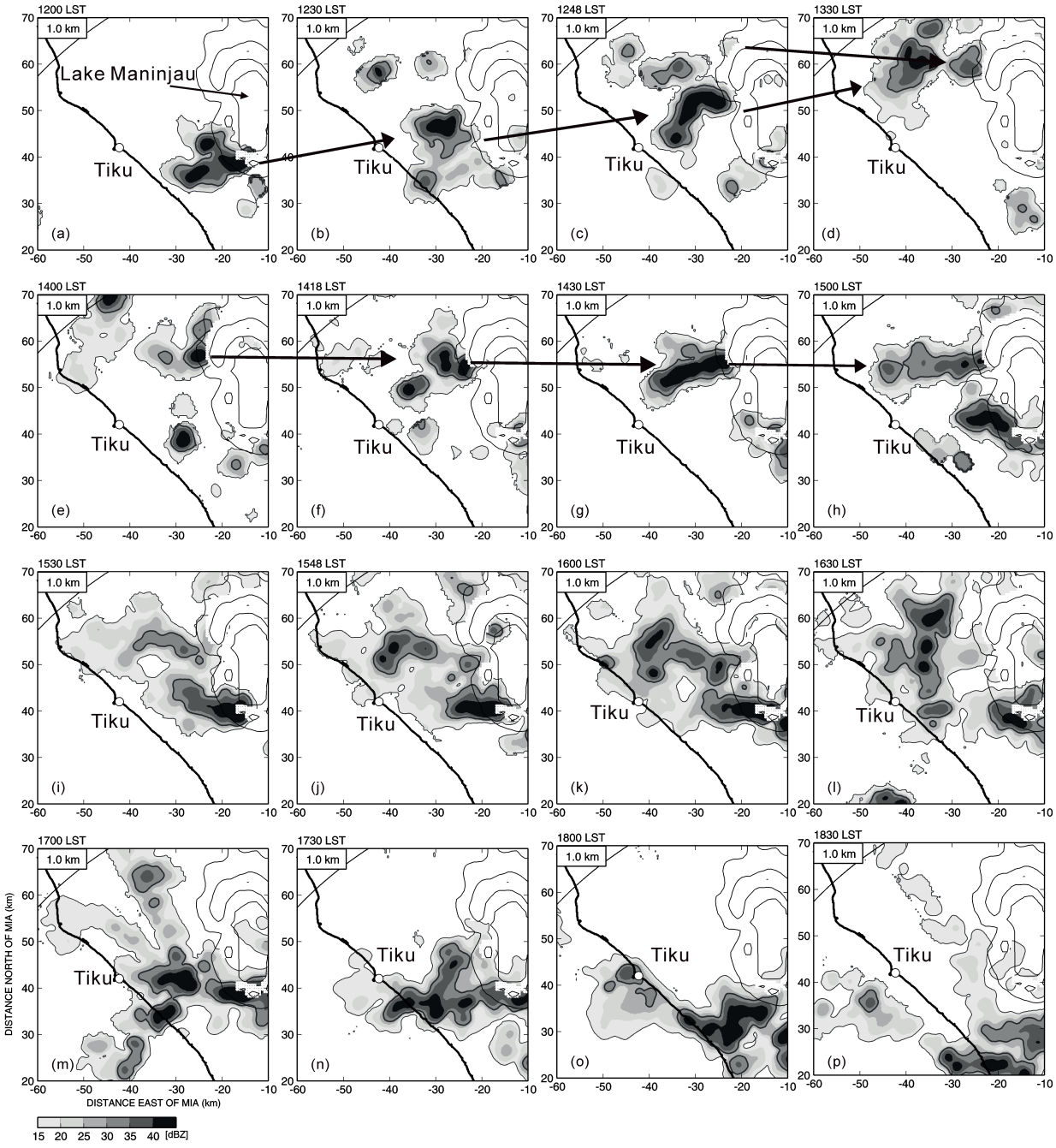

Fig. 5. As for Fig. 4, but from 1200 to 1830 LST on 10 November 2006.

2003) that appear to be related to annual variations (i.e., a north-south shift about the equator) in the intertropical convergence zone (ITCZ) (Murakami and Matsumoto 1994; Okamoto et al. 2003). However, the period of HARIMAU2006 coincided with a positive phase of an Indian Ocean Dipole Zonal Mode event and weak to moderate-strength El Nino, meaning that convection was suppressed in the warm pool regions of the eastern Indian Ocean and western Pacific (McPhaden 2008; Yoneyama et al. 2008). Figure

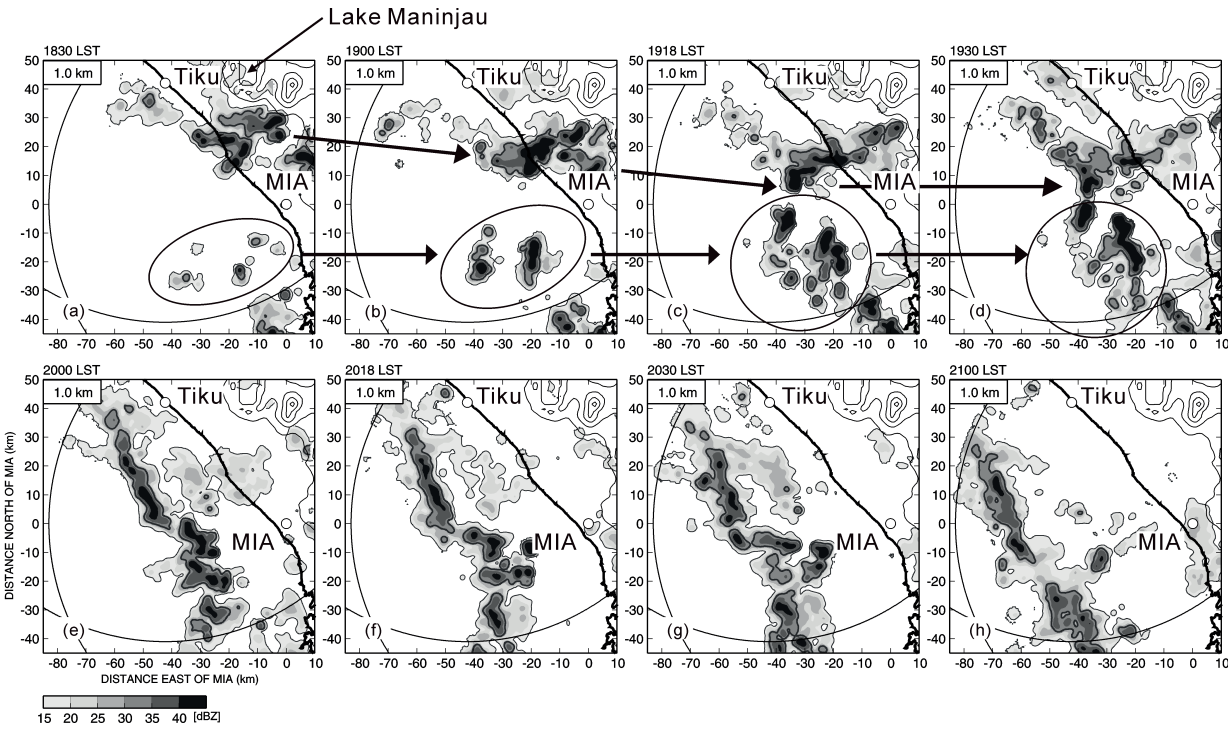

Fig. 6. As for Fig. 4, but from 1830 to 2100 LST on 10 November 2006.

2 shows a time-longitude cross-section of black body temperature (T_{BB}) by Multi-functional Transport Satellite (MTSAT) IR1. Despite the fact that observations were made during a period of suppressed convective activity, a diurnal cycle of convective activity occurred almost every day and the westward migration of cloud systems was commonly observed in central Sumatera during HARIMAU2006.

The typical diurnal cycle of westward migration of cloud systems was observed on 10 November 2006. Figure 3 shows the horizontal distribution of T_{BB}. Convection became active ($T_{BB} \leq 230$ K) from 1300 LST (data not shown) and cloud systems grew to several hundred kilometers in horizontal extent over the west coast of Sumatera Island by 1600 LST. The cloud systems then migrated westward; the core of the systems had moved offshore by 2000 LST. At 0000 LST on 11 November, the core of the cloud systems was located over offshore islands, approximately 150 km from the west coast of Sumatera Island.

3.2 Temporal variations in the horizontal distribution of precipitation systems

The migration of precipitation systems observed by XDR was more complicated than that of cloud systems observed by MTSAT IR1. Figures 4 and 5 show temporal variations in the horizontal distribution of precipitation systems at a height of 1.0 km from 1012 to 1830 LST on 10 November 2006. An isolated convective cell was generated near the west coast of Sumatera Island about 20 km from the south slope of Lake Maninjau (LM) at 1012 LST (Fig. 4a). New convective cells were sequentially initiated toward the south slope of LM, and a convective cell was generated over the south slope of LM at 1036 LST (Figs. 4b, c). The convective cell gradually intensified to a precipitation system with a horizontal scale of approximately 20 km, thereafter generating new convective cells in a westward direction and migrating to the southwest slope of LM by 1200 LST (Figs. 4d, 5a).

Between 1200 and 1800 LST, the precipitation systems changed their migration direction and shape several times over land, but they did not migrate to over the sea. From 1200 LST, a precipitation system migrated northwestward and left the area observed by the XDR located at MIA (Figs. 5a–e). At 1248 LST, a new convective cell developed over the northwest slope of LM and became organized into a precipitation system with a horizontal scale of approximately 10 km at around 1330 LST (Figs. 5c, d). The precipitation system mi-

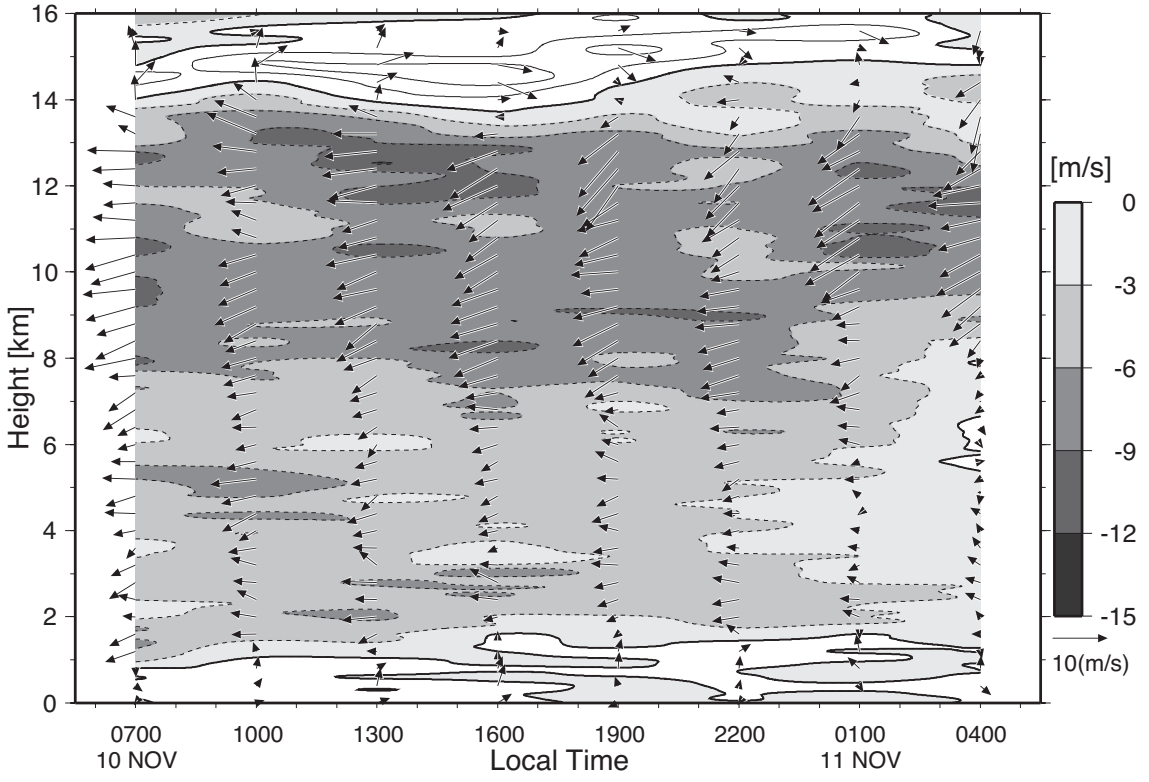

Fig. 7. Time-height cross-section of horizontal velocity (arrows; upward represents northward) from 0700 LST on 10 November to 0400 LST on 11 November 2006, as observed by rawinsondes launched at Tabing. Shading indicates zonal wind.

grated southwestward and merged with other precipitation systems, becoming organized into a line-shaped precipitation system at around 1430 LST (Figs. 5e–g). The line-shaped system remained west of LM for about 1 hour (Fig. 5h). From 1530 LST, the line-shaped system showed a change in shape to a wedge-shaped system west of LM (Figs. 5i–k). At 1630 LST, the wedge-shaped system again became a line-shaped system, aligned north-south (Fig. 5l). From 1630 LST, convective cells in the northern half of the line-shaped system migrated northward and decayed (Figs. 5m, n). In contrast, convective cells in the southern half of the system migrated eastward, merging with a precipitation system that had remained south of LM; the merged precipitation system changed its movement direction and migrated to over the sea (Figs. 5m–p).

Convective activity was initiated over the sea from 1830 LST (Fig. 6). New precipitation systems were generated over the sea and developed as they migrated northwestward (Figs. 6a–c). The precipitation systems that originated from over land and those generated over the sea became merged into a larger precipitation system than those over land (Figs. 6d, e). The expanded system migrated offshore (in a westward direction) from 1930 LST at a speed of about 5.0 m $s^{-1}$and left the area observed by XDRs at around 2200 LST (Figs. 6e–h). Mori et al. (2011) reported the monthly mean of the diurnal cycle in precipitation systems for the present study area: the precipitation area observed over land in daytime started to migrate toward the sea at around 1800 LST at a propagation speed of approximately 4.0 m s^{-1}. Thus, the present results are largely consistent with those of Mori et al. (2011), indicating that the case examined in the present study is typical of the diurnal cycle of convective activity in west Sumatera during HARIMAU2006.

3.3 Time variations in horizontal wind

Figure 7 shows a time-height cross-section of horizontal wind at Tabing obtained by 3-hourly rawinsonde observations on 10 November 2006. From 2 to 14 km in height, the easterly wind component was dominant

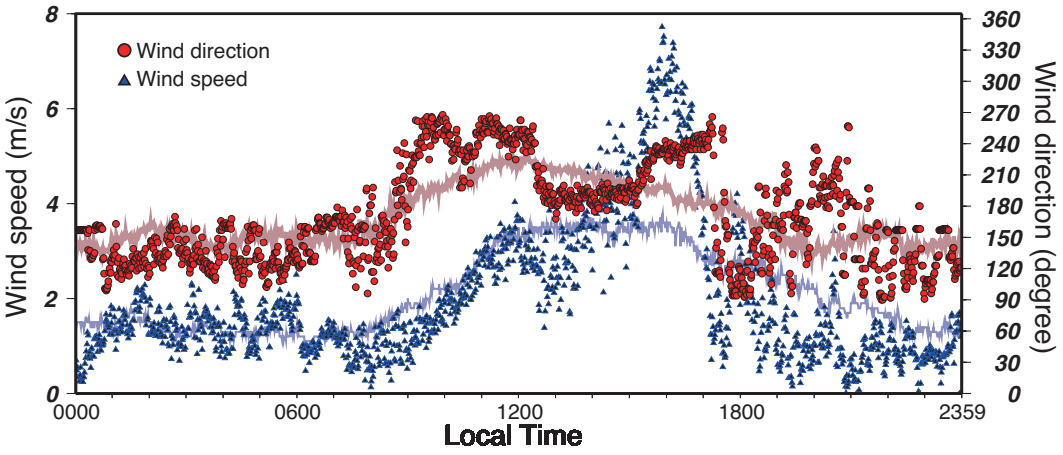

Fig. 8. Temporal variations in surface wind direction (red circles) and speed (blue triangles) at Tiku on 10 November 2006. Red and blue lines indicate monthly mean surface wind direction and speed, respectively.

and wind speed was stronger at higher altitudes. Local circulation was observed below 2 km in height with westerly (easterly) wind during the daytime (nighttime) below 1 km. Local circulation was also found in surface observations at Tiku (Fig. 8): southwesterly wind blew between 0800 and 1700 LST, subsequently changing to southeasterly. The surface wind speed gradually increased from 0800 LST, peaking at around 1600 LST (7.7 m s^{-1}) and rapidly decreasing thereafter. The surface wind speed during the nighttime was weak, generally less than 2.0 m s^{-1}. The surface wind speed and direction on 10 November 2006 at Tiku had a similar diurnal cycle to that of the monthly mean in November 2006, indicating that typical local circulation was observed on this day. Similar trends in surface wind were observed at MIA and Tabing (data not shown).

3.4 Precipitation systems over land

Subsection 3.2 described temporal variations in the migration of precipitation systems on 10 November 2006, revealing several changes in their migration directions and shapes during the daytime. We classified the migratory precipitation systems that occurred over land in the daytime into three phases as follows (the internal structure of the precipitation systems in each phase are described below):

1. Morning phase: isolated convective cells were generated near the west coast of Sumatera Island and propagated to mountainous areas via the self-replication of convective cells.

2. Afternoon phase: precipitation systems that developed over the slope of LM showed repeated changes in their migration directions and shapes.

3. Evening phase: precipitation systems migrated from land to sea.

Precipitation systems with various shapes and migration directions were assigned to the 2nd phase, as they shared a common origin over the slope of LM and they remained over land throughout their lifetimes. The internal structures of the various cases are not shown or compared in this paper, although the internal structure of one of the cases is described below.

During the 1st phase, an isolated convective cell was generated near the west coast at 1012 LST and new cells were successively generated toward the south slope of LM. Figure 9 shows the internal structure of convective cells at 1024 LST on 10 November 2006. Southeasterly wind was observed at a height of 2.0 km in a convective cell (Fig. 9a), and a similar horizontal wind field was observed at higher levels (data not shown). Southwesterly wind was observed at heights of 0.5 km (Fig. 9b) and 1.0 km in the convective cell (data not shown). Similarly, a southwesterly blew across the surface at Tiku (Fig. 8). A southwesterly wind turned to an updraft at the leading edge of the cell, and the updraft turned to a southeasterly above 2.0 km (Figs. 9a, c). During this phase, the echo-top height of the cells was relatively low ($\leq$6 km).

As a case of the 2nd phase, the internal structure and formation process of a line-shaped precipitation system over the west slope of LM, observed between 1248 and 1530 LST on 10 November 2006, is shown here. As outlined in Subsection 3.2, a convective cell was generated over the northwest slope of LM at 1248 LST and migrated southwestward to become a line-shaped precipi-

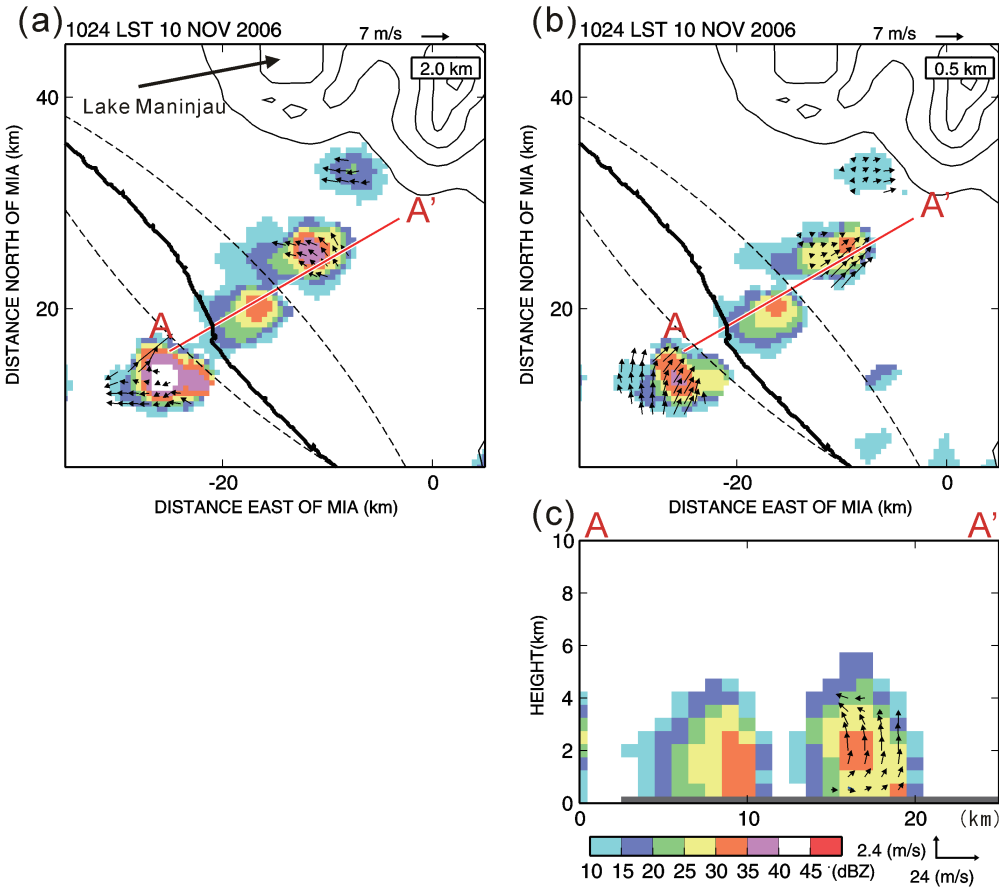

Fig. 9. Horizontal distributions of reflectivity and horizontal wind at heights of 2.0 km (a) and 0.5 km (b) and vertical cross-section of reflectivity and wind along line A-A′ (c) at 1024 LST on 10 November 2006. In (a) and (b), the thick line indicates the coastline and thin lines show altitude at intervals of 500 m. Dual-Doppler radar analysis was conducted within the overlapped area of the two solid circles shown in Fig. 1 and the area indicated by two dashed circles, except for the area in which the intersection angle is less than 30°. Gray shading in (c) indicates topography.

tation system between 1248 and 1430 LST (Figs. 5c–g). The line-shaped system was maintained between 1430 and 1530 LST (Fig. 5h). The echo-top height of the precipitation system was located at approximately 9 km (Figs. 10c–e). Southerly and southwesterly winds were dominant below 0.5 km (Figs. 8, 10a), whereas an easterly wind component was predominant at 2.0 km (Fig. 10b) and above this height (Fig. 7). Southerly wind in the lower troposphere struck the west slope of LM and turned to an updraft, and convective cells were generated over the west slope of LM. The convective cells were advected by the easterly wind, which was dominant above 2 km in height (Figs. 10c–e). The easterly wind turned to a downdraft over the adjacent plain, where the convective cells decayed there (Figs. 10c–e). This process continued to the west of LM and the line-shaped precipitation system was maintained for 1 hour.

During the 3rd phase, precipitation systems began to migrate from land to sea in the evening. Figure 11 shows the horizontal distribution of horizontal wind and reflectivity at a height of 0.5 km during 1600–1830 LST. Horizontal wind at 1600, 1630, and 1700 LST at a height of 0.5 km was directed toward LM (southerly, southwesterly, and westerly) and the precipitation systems remained over land. Some of the precipitation systems migrated from the plain located west of LM to the south slope of LM, as described in Subsection 3.2. From 1730 LST, horizontal wind started to blow from LM to the west coast, and the precipitation systems around LM started to move from LM to the west coast. At 1800

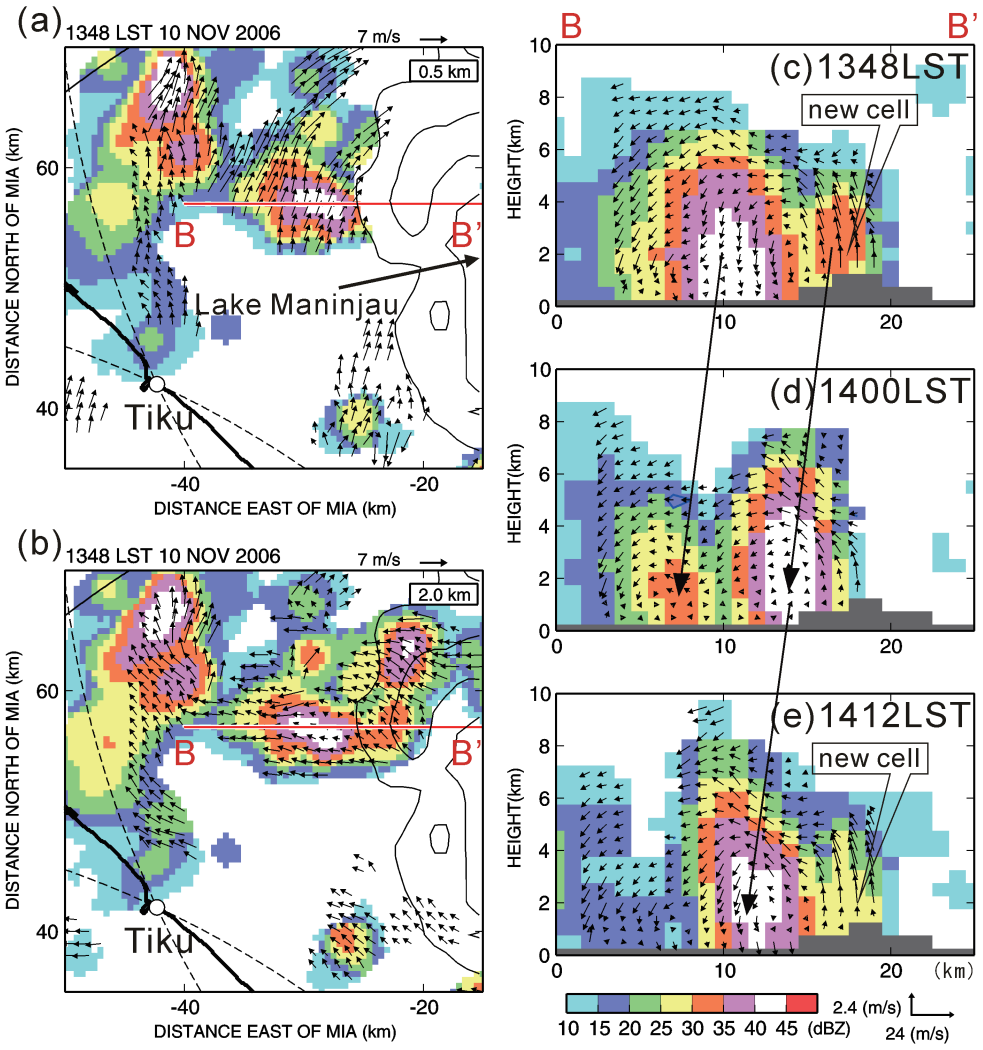

Fig. 10. Horizontal distributions of reflectivity and horizontal wind at heights of 0.5 km (a) and 2.0 km (b), and vertical cross-sections of reflectivity and wind along line B-B′ at 1348 LST (c), 1400 LST (d), and 1412 LST (e) on 10 November 2006. In (a) and (b), thick and thin lines indicate the coastline and altitude at intervals of 500 m, respectively. Dual-Doppler radar analysis was conducted within the overlapped area of the two solid circles (see Fig. 1) and the area indicated by two dashed circles, except for the area in which the intersection angle is less than 30°. Gray shading in (c)–(e) indicates topography.

and 1830 LST, northeasterly wind was dominant on the southwestern slope of LM. The surface wind at Tiku was southwesterly between 1600 and 1700 LST, changing to southeasterly between 1700 and 1800 LST, showing that the timing of the change in wind direction below 0.5 km corresponded to the timing of change in the migration direction of precipitation systems.

Here, we discuss the relationship between local circulation and the generation and migration of precipitation systems or convective cells over the land in daytime. During the 1st phase, direction along which new convective cell formed corresponded to the leeward side of horizontal wind in the lower layer. During the 2nd phase, the development of convective cells over the western slope of LM was influenced by the horizontal wind direction in the lower layer: the convective cells were generated by an updraft induced by local thermal circulation and the slope effect. On the other hand, the motion of the convective cells was affected by easterly wind in the upper layer. During the 3rd phase, the mi-

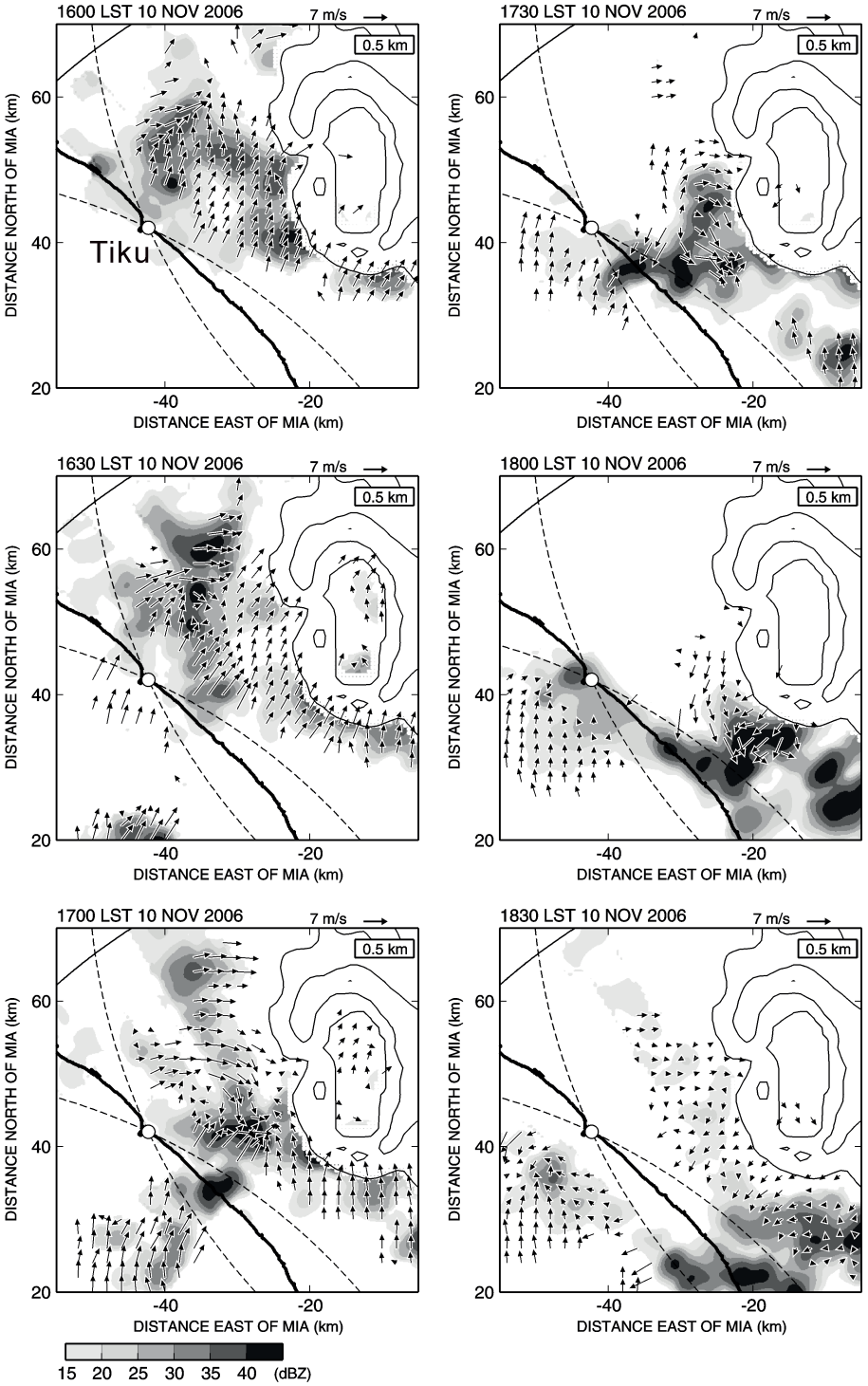

Fig. 11. Temporal variations in horizontal distribution of reflectivity and horizontal wind at a height of 0.5 km from 1600 to 1830 LST on 10 November 2006. Thick and thin lines indicate the coastline and altitude at intervals of 500 m, respectively. Dual-Doppler radar analysis was conducted within the overlapped area of the two solid circles (see Fig. 1) and the area indicated by two dashed circles, except for the area in which the intersection angle is less than 30°.

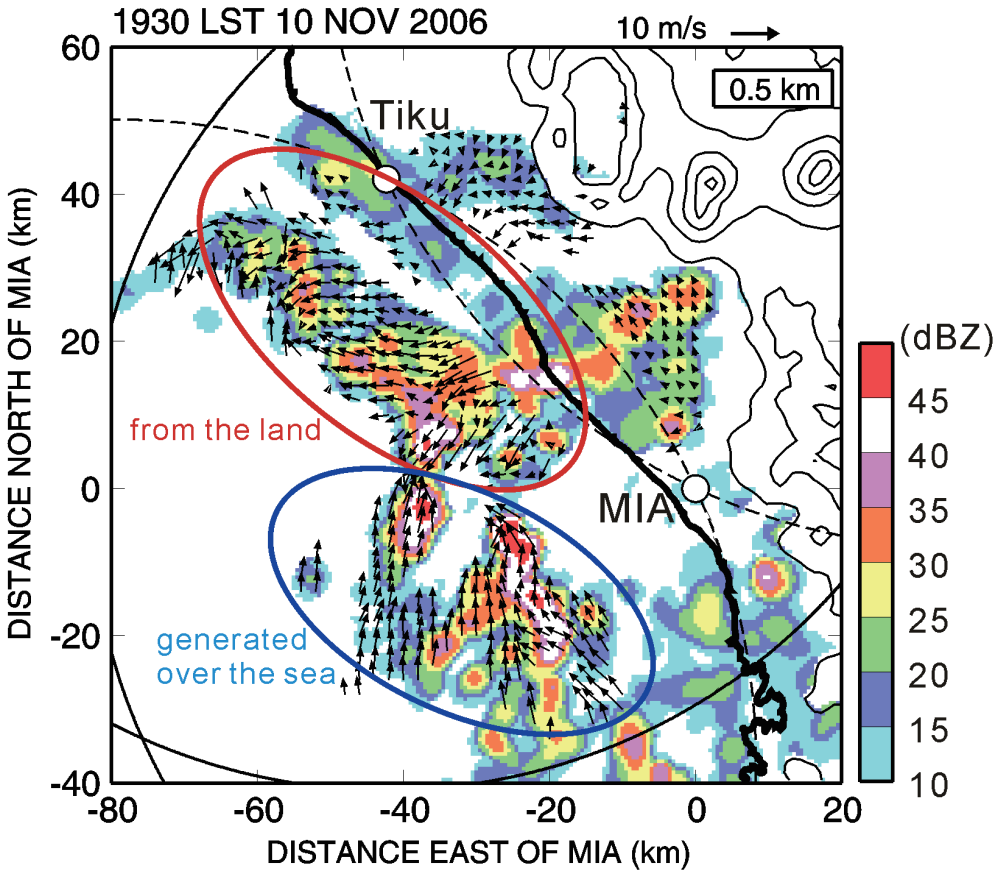

Fig. 12. Horizontal distribution of reflectivity and horizontal wind at a height of 0.5 km at 1930 LST on 10 November 2006. Thick and thin lines indicate the coastline and altitude at intervals of 500 m, respectively. Dual-Doppler radar analysis was conducted within the overlapped area of the two solid circles (see Fig. 1) and the area indicated by two dashed circles, except for the area in which the intersection angle is less than 30°.

gration direction of precipitation systems corresponded to the horizontal wind direction in the lower layer. The surface wind direction between 1024 and 1830 LST on 10 November 2006 at Tiku roughly corresponded to the horizontal wind direction at 0.5 km height observed by XDRs. Surface wind at Tiku on 10 November 2006 showed local circulation which was typical of that observed in November 2006, as mentioned in Subsection 3.3. Accordingly, it is proposed that local circulation affected not only the occurrence direction of new convective cells in the daytime, but also the timing of the evening change in the migration direction of precipitation systems from land to sea.

3.5 Precipitation systems over the sea

From 1830 LST, precipitation systems were generated over the sea near the west coastline and developed northwestward in association with southerly or southeasterly wind in the lower troposphere (Fig. 12). The precipitation systems from land migrated to the sea, accompanied by easterly or northeasterly wind in the lower troposphere (Fig. 12). These two sets of precipitation systems became merged into a much larger precipitation system than those over land, being greater than 100 km along the long axis and oriented parallel to the west coast of Sumatera Island (Fig. 13a). Figure 13 shows the horizontal distribution of reflectivity and horizontal wind at 2.0 km height, a vertical cross-section of reflectivity and wind, and mean profiles of zonal, meridional, and horizontal winds along line C-C′ in Fig. 13a at 1954 LST. The narrow convective region with a core of reflectivity exceeding 45 dBZ and oriented perpendicular to the west coast was observed at the leading edge of the precipitation system (Fig. 13b).

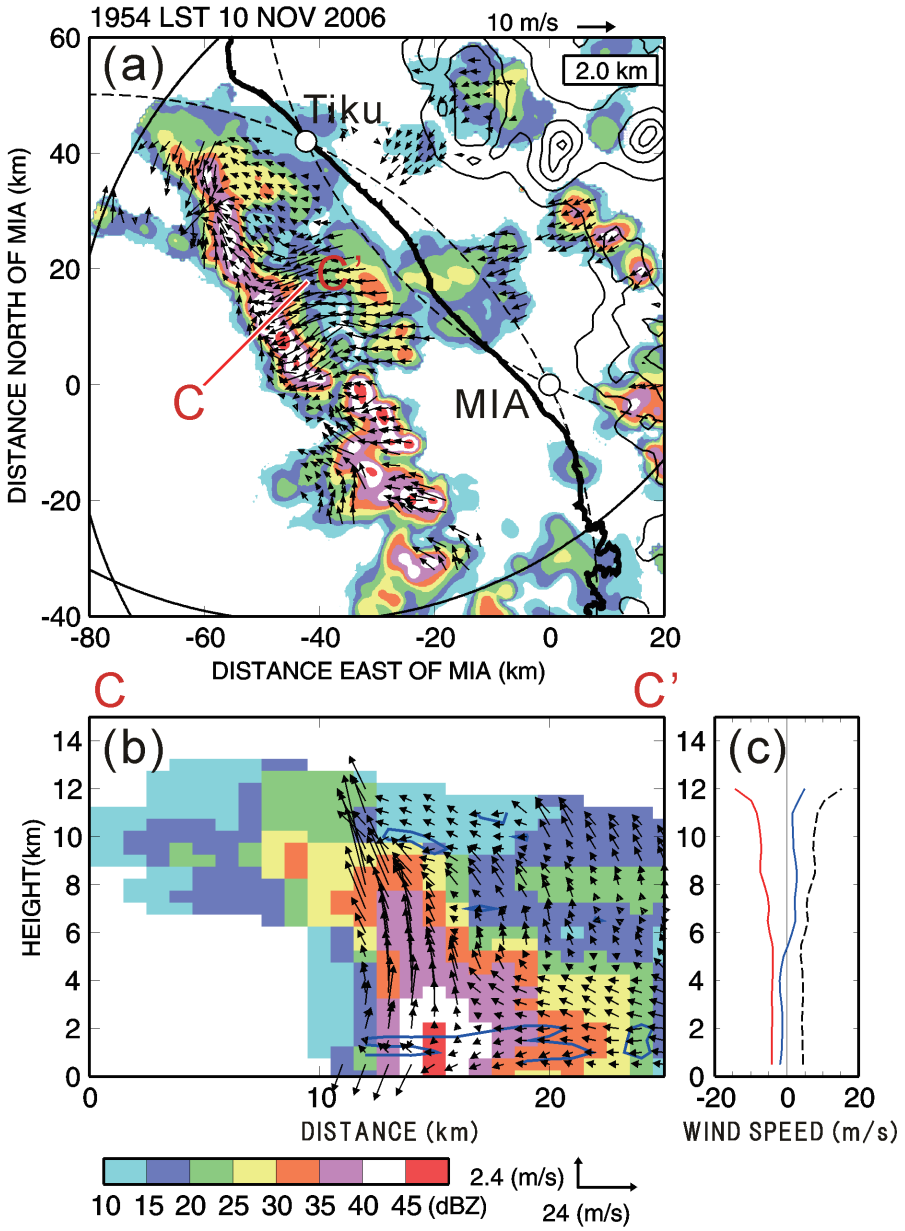

Fig. 13. The horizontal distribution of reflectivity and horizontal wind at a height of 2.0 km (a), a vertical cross–section of reflectivity and wind along line C-C′ (b), and mean profiles of zonal wind (red), meridional wind (blue), and horizontal wind (dashed) (c) at 1954 LST on 10 November 2006. Dual-Doppler radar analysis was conducted within the overlapped area of the two solid circles (see Fig. 1) and the area indicated by two dashed circles, except for the area in which the intersection angle is less than 30°. Blue contours in (b) indicate a vertical velocity of 0.0 m s^{-1}.

The width of the convective region with a reflectivity exceeding 35 dBZ was approximately 7 km at a height of 2.0 km (Figs. 13a, b). A downdraft was observed below 1.0 km at the leading edge of the precipitation system (Fig. 13b). A southerly inflow at a height of 2.0 km turned to an updraft above the downdraft (Figs. 13a, b). The updraft merged with ascending easterly wind from the weak echo region in the rear of the convective

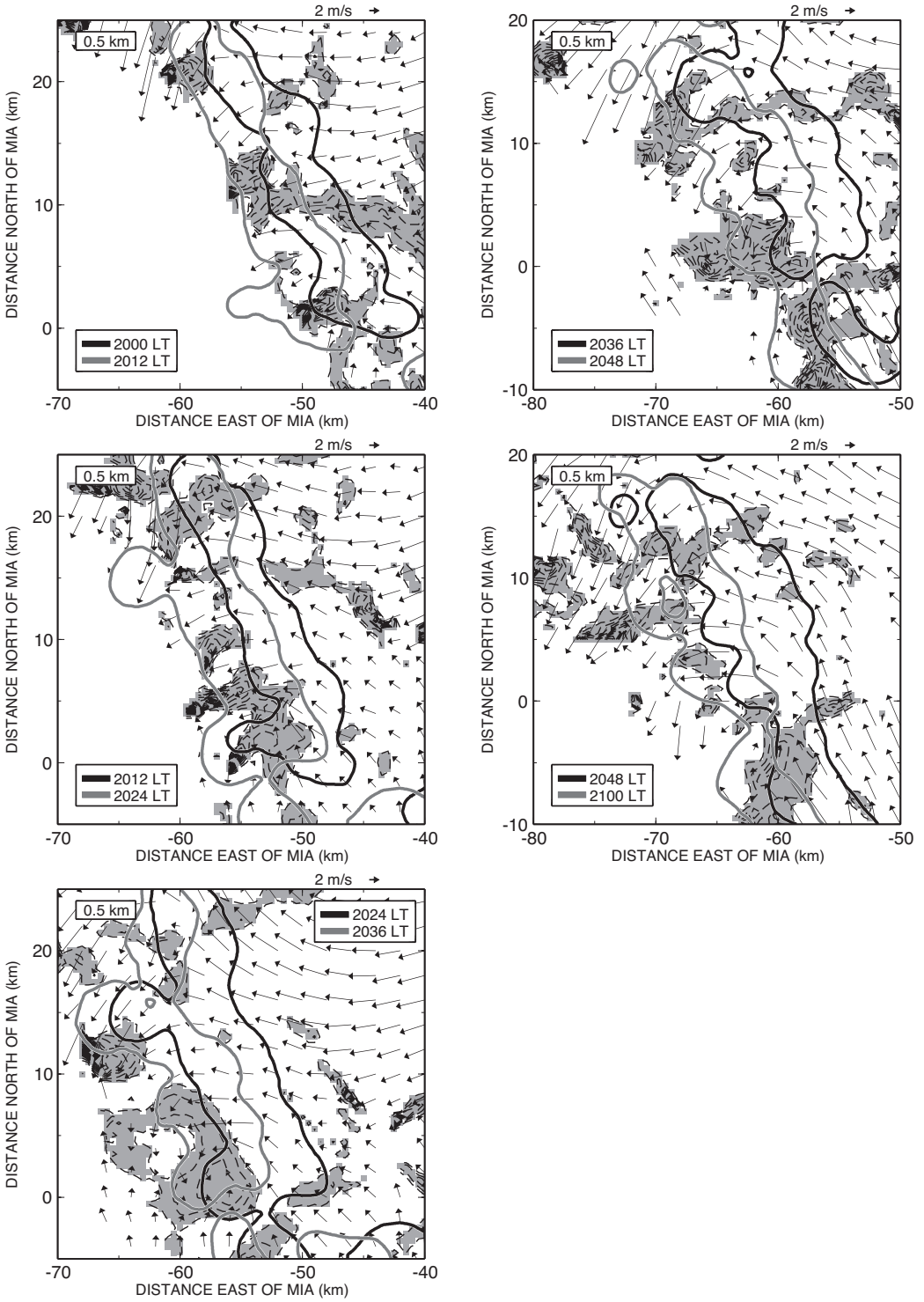

Fig. 14. Temporal variations in the horizontal distribution of a precipitation system, divergence, and horizontal wind at a height of 0.5 km from 2000 and 2100 LST on 10 November 2006. The thick black and gray contours are reflectivity greater than 30 dBZ. Thin dashed contour and gray shading indicate divergence less than -0.1×10^{-3} s^{-1}. Contour interval of the convergence is 0.5×10^{-3} s^{-1}.

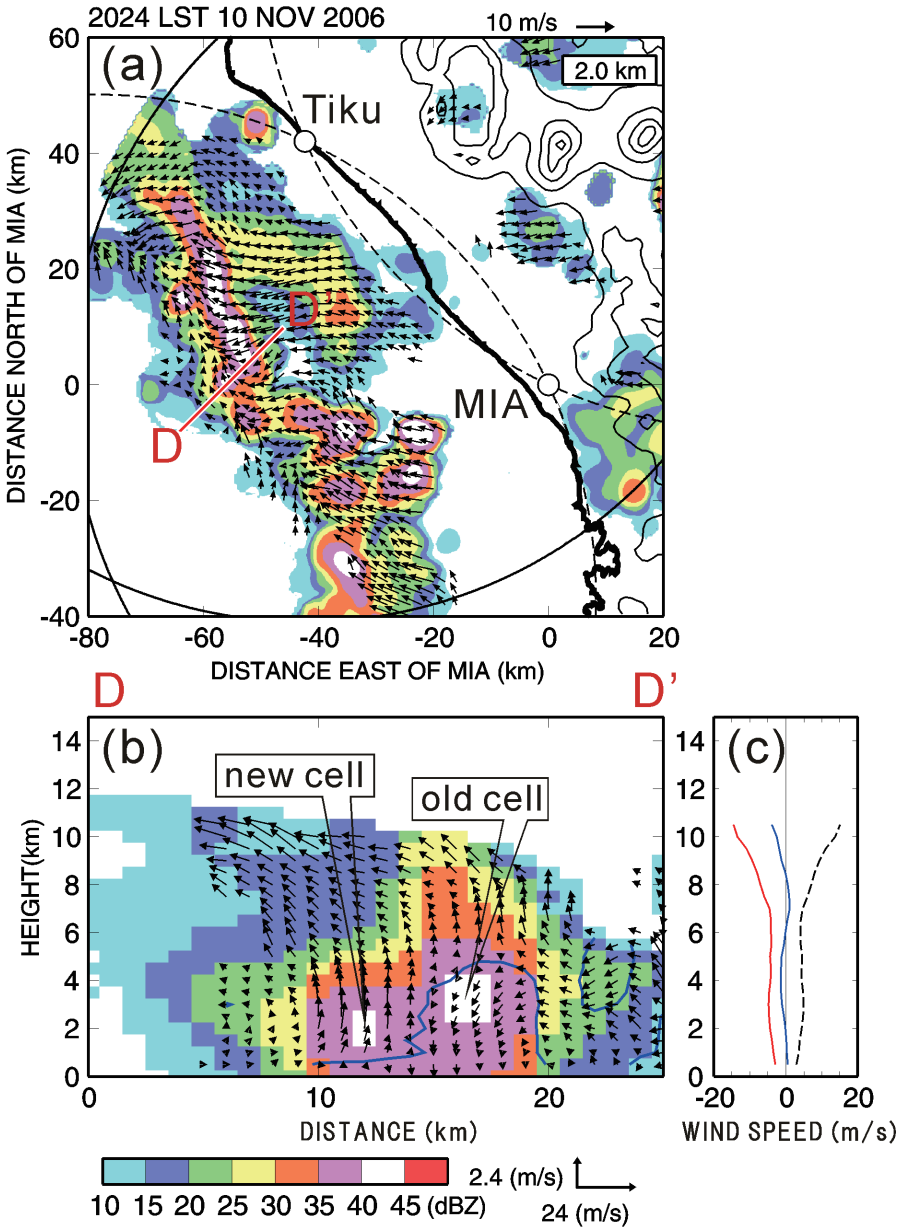

Fig. 15. As for Fig. 13, but for line D-D′ at 2024 LST.

region and had a peak of about 8 m s^{-1} at a height of 9 km (Fig. 13b). The echo-top height of the precipitation system was located at approximately 13 km (Fig. 13b). An anvil located above 6 km in height moved faster than the core of the convective region because of a strong easterly wind in the upper troposphere (Figs. 13b, c), as observed by rawinsondes (Fig. 7).

The migration process of the precipitation system over sea was investigated based on data from the two XDRs (Figs. 14, 15). Figure 14 shows the horizontal distribution of horizontal wind, divergence, and reflectivity at a height of 0.5 km from 2000 to 2100 LST on 10 November 2006. In the precipitation system, two migration processes were observed. In the first migration process, the system migrated westward maintaining its structure as shown in Fig. 13: horizontal wind converged at the leading edge of the system in the lower layer and a convective region was accompanied with an

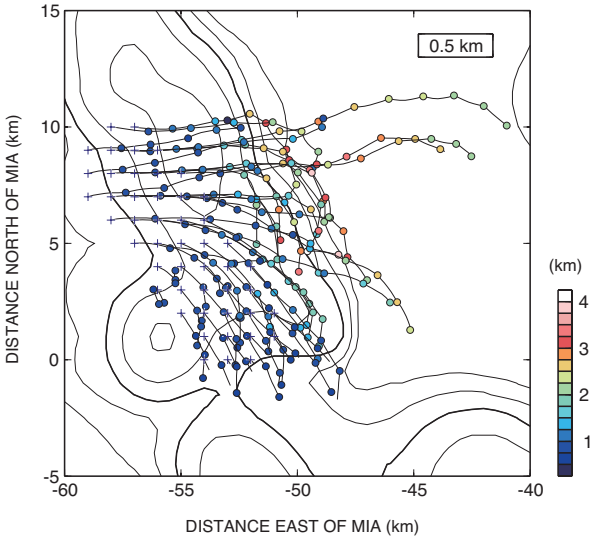

Fig. 16. Backward trajectory results for air parcels placed at a height of 0.5 km around the leading edge of the precipitation system at 2024 LST on 10 November 2006 (cross mark). Positions of the air parcels are plotted every 6 minutes by circle mark. Colors of the circle mark are heights of air parcels. Contours indicate reflectivity every 5 dBZ starting at 20 dBZ. Thick contour indicates reflectivity at 30 dBZ.

updraft above the convergence. Migration speed of this part was about 5 m s^{-1}, similar to the ambient wind speed in the lower troposphere (Figs. 7, 13b, c). In the second migration process, a new convective cell was generated at about 5 km ahead of the leading edge of the precipitation system (Fig. 14). Internal structure of the system in the second migration process is shown in Fig. 15. At 2024 LST, a new cell had developed with a core of reflectivity exceeding 40 dBZ at a height of 2.0 km in front of an old cell (Figs. 15a. b). An updraft was observed in the new cell and a downdraft was predominant below 5 km in height within the old cell (Fig. 15b). After the old cell decayed, the new cell became part of the precipitation system (Fig. 14). The precipitation system migrated via the above two migration processes at a speed of approximately 5 m s^{-1} from 1930 LST until around 2200 LST in the area observed by the XDRs (Fig. 14). Consequently, the migration mechanism of the precipitation system over the sea is considered to have been advection by ambient wind in the lower troposphere and self-replication of convective cells at the leading edge of the system.

These two migration mechanisms were considered to be concerned with the convergence in the lower troposphere. As shown in Fig. 14, the convergence region was mainly observed around leading edge of the precipitation system at the lowest layer. The convergence was formed by an easterly wind component in the system and a southerly wind component over the sea. The wind speed of the easterly wind component at the leading edge of the system was 4–6 m s^{-1}, which was larger than land breeze (less than 2.0 m s^{-1}). Therefore, the easterly wind component should be composed of not only land breeze but also other sources. Downdraft was also considered as possible formation mechanism of the easterly wind around the leading edge of the system at the lowest layer; however, the downdraft was weak during the dissipating stage of the convective cell, as shown in Fig. 15. Therefore, surface wind (land breeze) and downdraft alone are unable to explain the formation of the wind speed in the convergence region. We performed a trajectory analysis to investigate the formation mechanism of the convergence around the leading edge of the precipitation system (Fig. 16). Air parcels were placed at a height of 0.5 km around the leading edge of the system at 2024 LST and traced backward in time for 61 minutes. We assumed that the wind field was maintained for 6 minutes. The trajectory of air parcels was tracked using wind data renewed every minute. Air parcels were transported from east or southeast and from 4 km in height to the convergence region around the leading edge of the precipitation system at the lowest layer (Fig. 16). The ambient wind speed at around 4 km in height was 4–6 m s^{-1} (Figs. 7, 13c, 15c), similar to the wind speed in the convergence region observed by the two XDRs (Fig. 14). Therefore, we consider that downward transportation of horizontal momentum below 4 km also played an important role in intensifying the wind speed around leading edge of the system at the lowest layer. Since ambient easterly wind was predominant below 14 km on 10 November 2006 (Fig. 7), horizontal momentum below 4 km could be continuously transported downward, meaning that the system was maintained over the sea for a long time (more than 90 minutes) and migrated offshore for a long distance.

4. Discussion

As mentioned in the Introduction, little is known about the internal structure and migration process of a westward-migrating precipitation system with a diurnal cycle over the sea off Sumatera Island because, in a previous project (CPEA), an XDR was installed in mountainous terrain and did not cover the sea area off the west

coast of the island. In the present study, we aimed to fill gaps in our knowledge using data from two XDRs installed near the west coast of Sumatera Island, providing coverage of the sea off the west coast of the island. This section summarizes the internal structure and migration mechanism of a westward-migrating precipitation system with a diurnal cycle over the sea off the west coast of Sumatera Island. The results are then compared with the findings of previous studies in the region.

4.1 Internal structure of a westward-migrating precipitation system over the sea

In the present study, as shown in MTSAT image (Fig. 3), the horizontal scale of westward-migrating cloud systems with a diurnal cycle was several hundred kilometers over the sea, which is consistent with that of westward-migrating cloud systems shown in previous studies based on satellite data (Sakurai et al. 2005; Sakurai et al. 2009). Based on data from ground based radar data, we investigated the internal structure of a westward-migrating precipitation system over the sea and revealed that the precipitation system was much smaller than the cloud systems. The precipitation system had a convective region with a long axis ($>$100 km) oriented parallel to the west coast of Sumatera Island and a short axis ($\sim$7 km) oriented perpendicular to the coast. An anvil of the precipitation system moved faster than the convective region above 6 km in height (Fig. 13) and the echo top height of the precipitation system was located at approximately 13 km (Fig. 13). The precipitation system over the sea was much larger than that observed over land in the daytime (long axis of several tens of kilometers) because precipitation systems that originated from over land merged with those generated during the evening over the sea near the west coast of Sumatera Island (Fig. 11). These precipitation systems with different origins were accompanied by different winds in the lower layer: easterly or northeasterly wind in the precipitation systems from land and southerly or southeasterly wind in those generated over the sea (Fig. 12). Mori et al. (2011) described the evening-time expansion of the westward-migrating precipitation system over the sea, near the west coast of Sumatera Island based on monthly mean single radar data collected as part of HARIMAU2006. In the present study, the expansion process of the system was revealed for the first time based on dual-Doppler radar analysis.

We discuss the relationship between the expansion process of the precipitation system and abundant rainfall over the sea near the west coast of Sumatera Island. Previous studies on the climatological diurnal cycle of rainfall over Sumatera Island have shown that annual rainfall over the sea, near the west coast of the island, is much greater than that over the island itself, and that most of the rainfall over the sea occurs during nighttime (Hara et al. 2009; Mori et al. 2004; Wu et al. 2009). These earlier studies speculated that the abundant rainfall over the sea near west Sumatera is related to a westward-migrating precipitation system with a diurnal cycle. The results obtained in the present study support the speculation in these earlier studies: we revealed the expansion process of a westward-migrating precipitation system over the sea near the west coast of Sumatera Island. However, only one case was presented in the present study; further analyses are required to investigate if the expansion of the precipitation system examined in the present study is common to all systems in the region and to what degree the rainfall produced by the expanded system contributes to the abundant rainfall over the sea.

4.2 Mechanism of westward migration of the precipitation system over the sea

In the case analyzed in the present study, a precipitation system located over the mountains of Sumatera Island started migrating to the sea in association with a change in local circulation from landward to seaward at around 1730 LST (Fig. 11). After the system merged with other system generated over the sea near the west coast, the system migrated further offshore via two mechanisms. The first migration mechanism is advection by ambient wind in the lower troposphere because the migration speed of the precipitation system over the sea was about 5 m s^{-1}, similar to that of ambient wind in the lower troposphere where the easterly wind component was dominant above 2 km. During the advection by ambient easterly wind in the lower troposphere, a convergence in the lower layer and an updraft above the convergence were maintained in convective region in the system. The second mechanism is successive generation of convective cells at the leading edge of the system (Fig. 15) arising from convergence between an easterly wind component from the dissipating stage of the convective cell and the ambient southerly wind over the sea in the lower layer (Figs. 14, 15). The convergence at the leading edge of the system played an important role in these two migration mechanisms. We suggested that the main factor behind convergence formation at the leading edge of the system was the downward transportation of horizontal momentum below 4 km because air parcels at the lowest layer at the leading edge of the system were transported from 4 km in height (Fig. 16) and the ambient wind speed and direction below 4 km were similar to the wind speed and di-

rection in the lower layer at the leading edge of the system (Figs. 7, 14, 15). This view is also supported by the observation that the land breeze ($\sim$2 m s^{-1}) and downdraft from the dissipating stage of the convective cell were too weak to explain the wind speed in the lower layer at the leading edge of the system (Figs. 8, 15).

The above mechanisms of the westward-migration of the precipitation system are now compared with the results of previous studies. The first migration mechanism (i.e., advection by ambient wind in the lower troposphere) is consistent with the mechanism proposed in previous studies that considered ground-based radar data (Mori et al. 2011; Sakurai et al. 2009). The second migration mechanism (i.e., the successive generation of convective cells at the leading edge of the precipitation system) is also consistent with the mechanism proposed in previous studies (Mori et al. 2011; Sakurai et al. 2009; Wu et al. 2009). However, there is a difference in the type of the wind that converges with ambient wind in the lower layer: in the present study, not only land breeze and downdrafts from old convective cell, but also downward transportation of horizontal momentum below 4 km strengthen the convergence in the lower layer at the leading edge of the system. Whereas in Mori et al. (2011), a land breeze is the main component of the wind that converges with ambient wind in the lower layer, and Wu et al. (2009) emphasized the role of a gust derived from an old convective cell. In summary, the two migration mechanisms proposed in the present study to explain the westward migration of precipitation system are consistent with the mechanisms proposed in previous studies, which suggests these are the main mechanisms of migration in west Sumatera. However, there are conflicting ideas regarding the type of wind that converges with ambient wind in the lower layer. Consequently, some questions remain in terms of the westward migration mechanism. Further studies are required to answer these questions, including case studies based on observational data and sensitivity experiments using numerical models.

5. Conclusion

This study examined the internal structure and migration process of a westward-migrating precipitation system with a diurnal cycle observed on 10 November 2006 in west Sumatera based on dual-Doppler radar analysis, rawinsonde data, and surface data obtained as part of HARIMAU2006, along with MTSAT IR1 data. The location of convective cell generation over land in the daytime and the timing of evening changes in the migration direction of precipitation systems from landward to seaward were influenced by local circulation: in the morning, an isolated convective cell was generated near the west coast and new convective cells were successively generated over the sea breeze (Figs. 4, 9). In the afternoon, precipitation systems showed repeated changes in migration direction and shape over land (Fig. 5). A case study of precipitation systems observed over land in the afternoon revealed that convective cells in a precipitation system were successively generated over the western slopes of the mountains surrounding Lake Maninjau (LM) by thermally induced local circulation and by the slope effect (Fig. 10); the precipitation system was maintained for 1 hour (Figs. 5g, h). From 1730 LST, a mountain breeze started to blow from LM toward the west coast, resulting in migration of the system toward the sea (Fig. 11).

From 1830 LST, precipitation systems began generation over the sea near the west coastline of the island (Fig. 6a). The systems generated over the sea and those migrating from land merged to produce a larger precipitation system than those over land (Figs. 6b–e, 12). The expanded precipitation system had a convective region with a long axis oriented parallel to the west coast of the Island ($>$100 km) and a short axis ($\sim$7 km) oriented perpendicular to the west coast at the leading edge of the system (Fig. 13). The echo top height of the system was located at approximately 13 km and an anvil moved faster than the convective region above 6 km in height. After 1930 LST, the system migrated farther offshore at a speed of about 5 m s^{-1}, similar to the ambient wind direction and speed in the lower troposphere (Figs. 6d–h). The mechanisms of migration for the system over the sea were advection by ambient wind in the lower troposphere and the successive generation of convective cells at the leading edge of the system (Fig. 14). We consider that continuous downward transportation of horizontal momentum below 4 km strengthened the convergence at the leading edge of the system, resulting in the maintenance of the system over the sea for a long time and the migration over the sea for a long distance (Fig. 16).

Migrating precipitation systems associated with a diurnal cycle in west Sumatera have been investigated previously in terms of their climatological characteristics based mainly on long-term satellite data (Mori et al. 2004; Murakami 1983; Nitta and Sekine 1994; Sakurai et al. 2005; Yang and Slingo 2001). The CPEA and HARIMAU projects made use of ground-based observations by XDRs, yielding three-dimensional data with high spatial and temporal resolution, which provided an advance in our understanding of the diurnal cycle of migrating precipitation systems in the west Sumatera region. The present study is the first to document the three-dimensional structure of the wind field and the mi-

gration process of precipitation systems associated with a diurnal cycle in the region. Because we presented only a single case study, it is necessary to perform additional case studies under different atmospheric conditions (e.g., ambient wind speed and direction, season, and phase of intraseasonal variation) in order to obtain a comprehensive understanding of the three-dimensional structure and migration process of migrating precipitation systems with a diurnal cycle in this region. Another intensive observation campaign, employing dual Doppler radar, was conducted during April and May of 2007 in the same area as that considered in the present study, also the XDR at MIA is now operating as part of the HARIMAU project, producing data for future analyses.

Acknowledgements

The HARIMAU project was supported by the Japan Earth Observing System (EOS) Promotion Program (JEPP) of the Ministry of Education, Culture, Sports, Science and Technology (MEXT) of Japan. Data used in this study such as the two XDRs at MIA and Tiku, rawinsondes at Tabing, and the surface wind data at Tiku were obtained by the HARIMAU project. We heartily thank colleagues at the Agency for the Assessment and Application of Technology (BPPT), BMG, and the National Institute of Aeronautics and Space (LAPAN) on the Indonesian-side, and the Japan Agency for Marine-Earth Science and Technology (JAMSTEC), Hokkaido University, and Kyoto University on the Japanese-side for their strong collaborations in performing observations. We would also like to thank Dr. Takeshi Maesaka of the National Research Institute for Earth Science and Disaster Prevention (NIED) for many useful suggestions regarding the analysis of radar data. Thanks are also extended to the constructive comments of the Editor (Prof. Takehiko Satomura) and two anonymous reviewers who greatly improved the content of this manuscript. Dr. Tokio Kikuchi of Kochi University is thanked for providing MTSAT IR1 data. Figures were drawn using Grid Analysis and Display System (GrADS) and Generic Mapping Tools (GMT).

References

Arakawa, O., and A. Kitoh, 2005: Rainfall diurnal variation over the Indonesian maritime contient simulated by 20 km-mesh GCM. *SOLA*, **1**, 109–112.

Cressman, G. P., 1959: An operational objective analysis system. *Mon. Wea. Rev.*, **87**, 367–374.

Fudeyasu, H., K. Ichiyanagi, K. Yoshimura, S. Mori, N. Sakurai, J.-I. Hamada, M. D. Yamanaka, J. Matsumoto, and F. Syamsudin, 2011: Effects of large-scale moisture transport and mesoscale processes on precipitation isotope ratios observed at Sumatera, Indonesia. *J. Meteor. Soc. Japan*, **89A**, 49–59.

Fujita, M., K. Yoneyama, S. Mori, T. Nasuno, and M. Satoh, 2011: Diurnal convection peaks over the eastern Indian ocean off Sumatra during different MJO phases. *J. Meteor. Soc. Japan*, **89A**, 317–330.

Fukao, S., 2006: Coupling processes in the Equatorial atmosphere (CPEA): A project overview. *J. Meteor. Soc. Japan*, **84A**, 1–18.

Hamada, J.-I., 2003: A climatological study on rainfall variations over the Indonesian maritime continent. Doctoral thesis, Graduate School of Science, Kyoto University, 189pp.

Hara, M., T. Yoshikane, H. G. Takahashi, F. Kimura, A. Noda, and T. Tokioka, 2009: Assessment of the diurnal cycle of precipitation over the maritime continent simulated by a 20 km mesh GCM using TRMM PR data. *J. Meteor. Soc. Japan*, **87A**, 413–424.

Hendon, H. H., and K. Woodberry, 1993: The diurnal cycle of tropical convection. *J. Geophys. Res.*, **98**, 16,623–16,637.

Kawashima, M., Y. Fujiyoshi, M. Ohi, T. Honda, T. Kozu, T. Shimomai, and H. Hashiguchi, 2006: Overview of Doppler radar observations of precipitating cloud systems in Sumatera Island during the first CPEA campaign. *J. Meteor. Soc. Japan*, **84A**, 33–56.

Kawashima, M., Y. Fujiyoshi, M. Ohi, S. Mori, N. Sakurai, Y. Abe, W. Harjupa, F. Syamsudin, and M. D. Yamanaka, 2011: Case study of an intense wind event associated with a mesoscale convective system in west Sumatera during the HARIMAU2006 campaign. *J. Meteor. Soc. Japan*, **89A**, 239–257.

McPhaden, M. J., 2008: Evolution of the 2006–2007 El Nino: The role of intraseasonal to interannual time scale dynamics. *ADGEO*, **14**, 219–230.

Mori, S., J.-I. Hamada, Y. I. Tauhid, M. D. Yamanaka, N. Okamoto, F. Murata, N. Sakurai, H. Hashiguchi, and T. Sribimawati, 2004: Diurnal land-sea rainfall peak migration over Sumatera Island, Indonesian maritime continent observed by TRMM satellite and intensive rawinsonde soundings. *Mon. Wea. Rev.*, **132**, 2021–2039.

Mori, S., J.-I. Hamada, N. Sakurai, H. Fudeyasu, M. Kawashima, H. Hashiguchi, F. Syamsudin, A. A. Arbain, R. Sulistyowati, J. Mastumoto, and M. D. Yamanaka, 2011: Convective systems developed along the coastline of Sumatera Island, Indonesia, observed with an X-band Doppler radar during the HARIMAU2006 campaign. *J. Meteor. Soc. Japan*, **89A**, 61–81.

Murakami, M., 1983: Analysis of the deep convective activity over the western Pacific and Southeast Asia. Part I: Diurnal variation. *J. Meteor. Soc. Japan*, **61**, 60–76.

Murakami, T., and J. Matsumoto, 1994: Summer monsoon over the Asian continent and western north Pacific. *J. Meteor. Soc. Japan*, **72**, 719–745.

Neal, R., and J. Slingo, 2003: The maritime continent and its role in the global climate: a GCM study. *J. Climate*, **16**, 834–848.

Nitta, T., and S. Sekine, 1994: Diurnal variation of convective activity over the tropical western Pacific. *J. Meteor. Soc. Japan*, **72**, 627–641.

Okamoto, N., M. D. Yamanaka, S.-Y. Ogino, H. Hashiguchi, N. Nishi, T. Sribimawati, and A. Numaguti, 2003: Seasonal variations of tropospheric wind over Indonesia: Comparison between collected operational rawinsonde data and NCEP reanalysis for 1992–99. *J. Meteor. Soc. Japan*, **81**, 829–850.

Ramage, C. S., 1968: Role of a tropical "maritime continent" in the atmospheric circulation. *Mon. Wea. Rev.*, **96**, 365–370.

Sakurai, N., F. Murata, M. D. Yamanaka, S. Mori, J.-I. Hamada, H. Hashiguchi, Y. I. Tauhid, T. Sribimawati, and B. Suhardi, 2005: Diurnal cycle of cloud system migration over Sumatera Island. *J. Meteor. Soc. Japan*, **83**, 835–850.

Sakurai, N., M. Kawashima, Y. Fujiyoshi, H. Hashiguchi, T. Shimomai, S. Mori, J.-I. Hamada, F. Murata, M. D. Yamanaka, Y. I. Tauhid, T. Sribimawati, and B. Suhardi, 2009: Internal structures of migratory cloud systems with diurnal cycle over Sumatera Island during CPEA-I campaign. *J. Meteor. Soc. Japan*, **87**, 157–170.

Sato, T., H. Miura, M. Satoh, Y. N. Takayabu, and Y. Wang, 2009: Diurnal cycle of precipitation in the tropics simulated in a global cloud-resolving model. *J. Climate*, **22**, 4,809–4,826.

Shimizu, S., H. Uyeda, Q. Moteki, T. Maesaka, Y. Takaya, K. Akaeda, T. Kato, and M. Yoshizaki, 2008: Structure and formation mechanism on the 24 May 2000 supercell-like storm developing in a moist environment over the Kanto Plain, Japan. *Mon. Wea. Rev.*, **136**, 2,389–2,407.

Wu, P., M. Hara, J.-I. Hamada, M. D. Yamanaka, and F. Kimura, 2009: Why a large amount of rain falls over the sea in the vicinity of western Sumatra Island during nighttime. *J. Appl. Meteor. Climatol.*, **48**, 1,345–1,361.

Yamanaka, M. D., H. Hashiguchi, S. Mori, P.-M. Wu, F. Syamsudin, T. Manik, J.-I. Hamada, M. K. Yamamoto, M. Kawashima, Y. Fujiyoshi, N. Sakurai, M. Ohi, R. Shirooka, M. Katsumata, Y. Shibagaki, T. Shimomai, Erlansyah, W. Setiawan, B. Tejasukmana, Y. S. Djajadihardja, and J. T. Anggadiredja, 2008: HARIMAU radar-profiler network over the Indonesian maritime continent: A GEOSS early achivement for hydrological cycle and disaster prevention. *J. Disaster Research*, **3**, 78–88.

Yang, G. Y., and J. Slingo, 2001: The diurnal cycle in the Tropics. *Mon. Wea. Rev.*, **129**, 784–801.

Yoneyama, K., Y. Masumoto, Y. Kuroda, M. Katsumata, K. Mizuno, Y. N. Takayabu, M. Yoshizaki, A. Shareef, Y. Fujiyoshi, M. J. McPhaden, V. S. N. Murty, R. Shirooka, K. Yasunaga, H. Yamada, N. Sato, T. Ushiyama, Q. Moteki, A. Seiki, M. Fujita, K. Ando, H. Hase, I. Ueki, T. Horii, C. Yokoyama, and T. Miyakawa, 2008: MISMO field experiment in the equatorial Indian ocean. *Bull. Amer. Meteor. Soc.*, **89**, 1,889–1,903.